INVENTORY OF SUPPLEMENTAL INFORMATION

SUPPLEMENTAL FIGURES

Sarosiek et al., Supplemental Figure S1

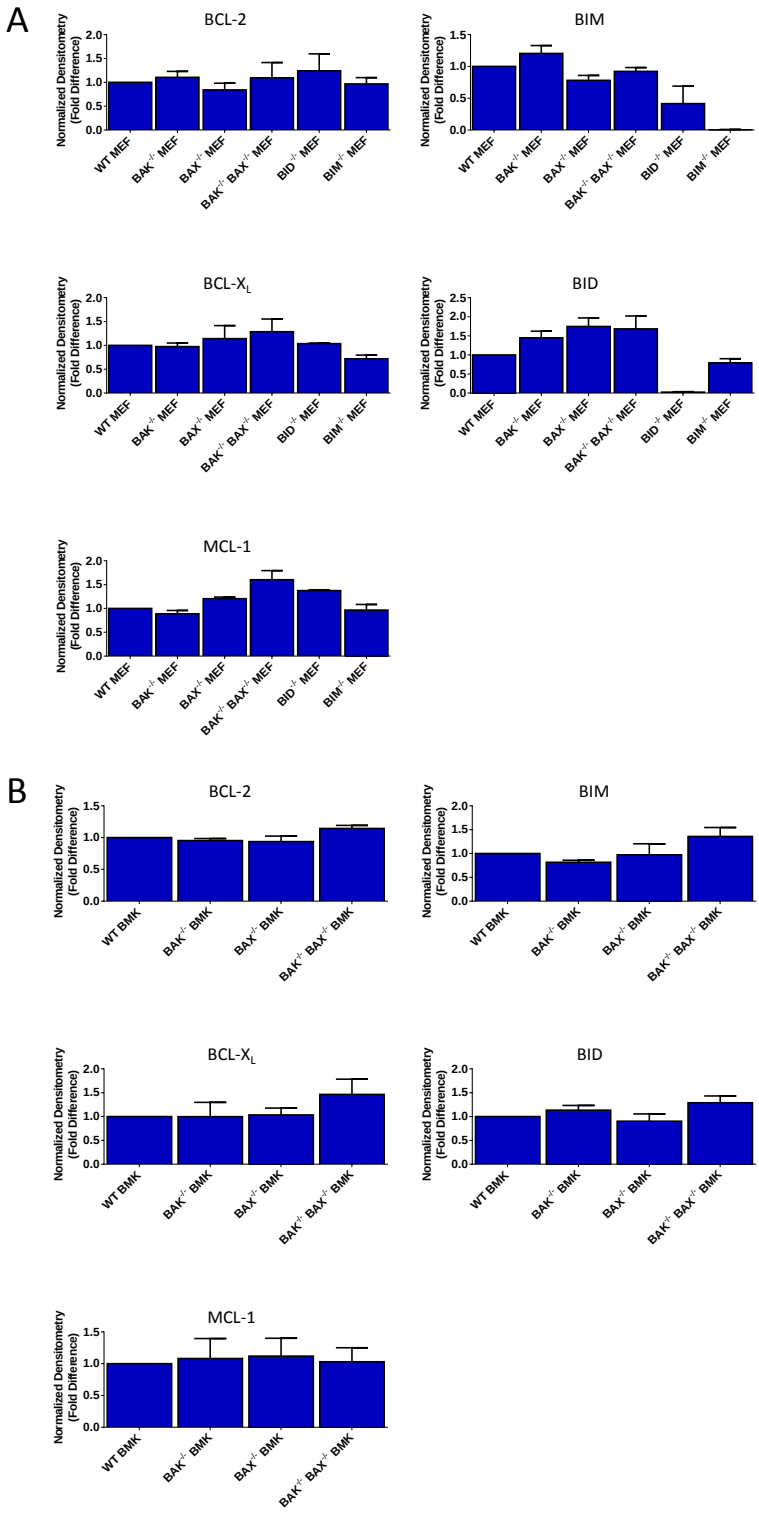

Sarosiek et al., Supplemental Figure S2

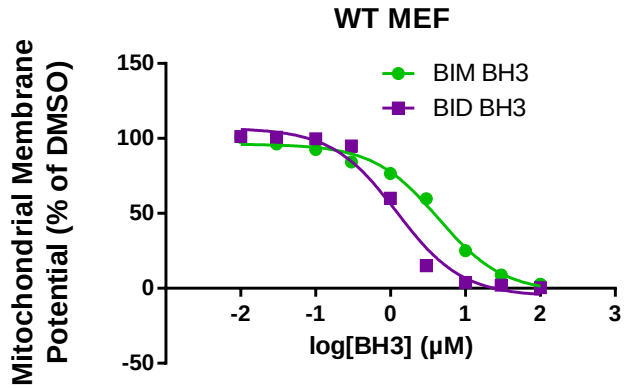

Sarosiek et al., Supplemental Figure S3

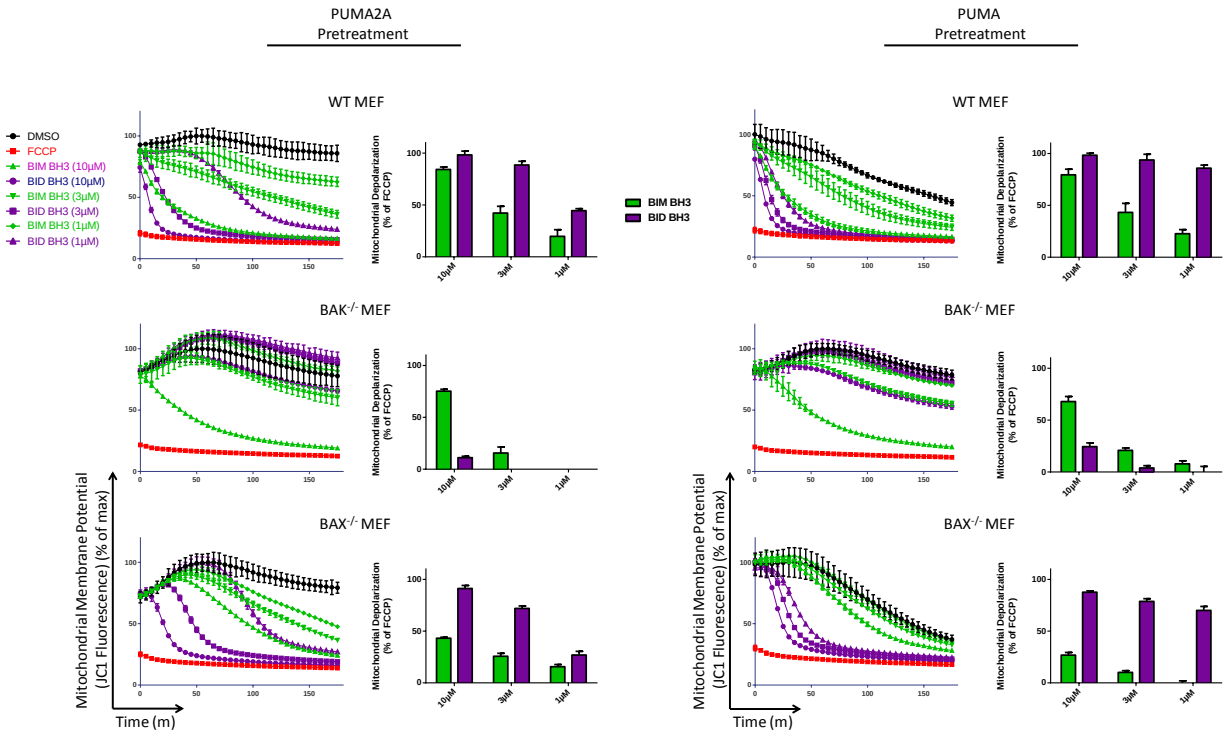

Sarosiek et al., Supplemental Figure S4

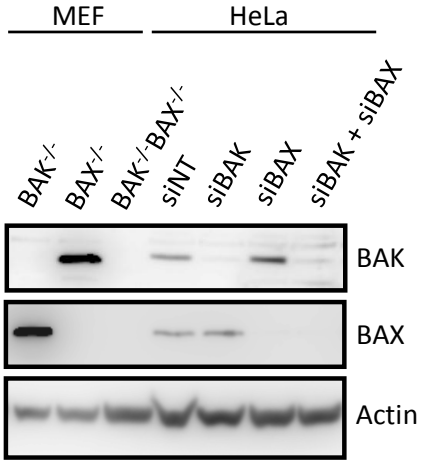

Sarosiek et al., Supplemental Figure S5

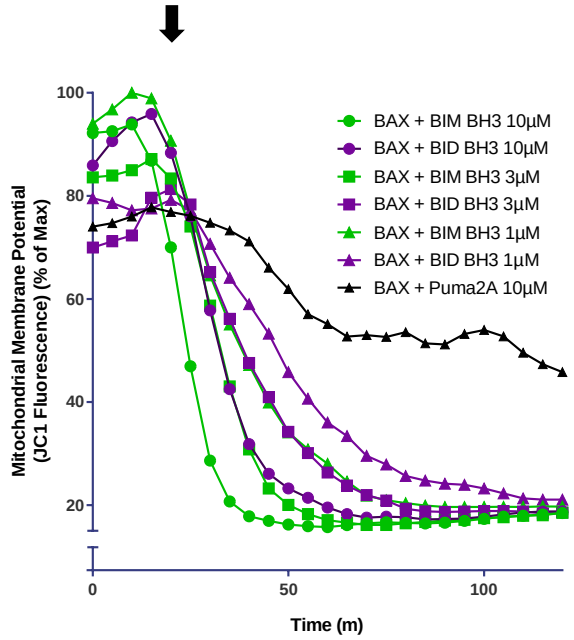

Sarosiek et al., Supplemental Figure S6

WT MEF

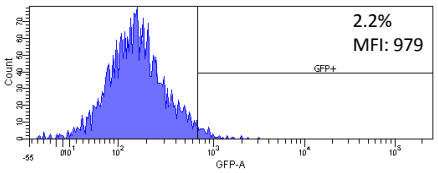

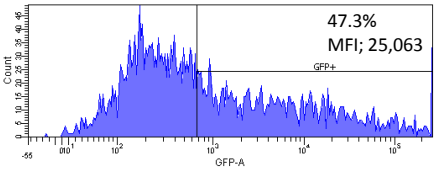

$BAK^{-/-}$ MEF

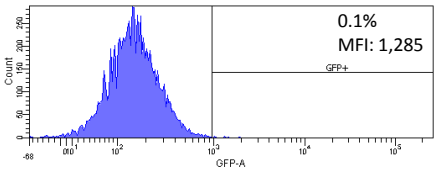

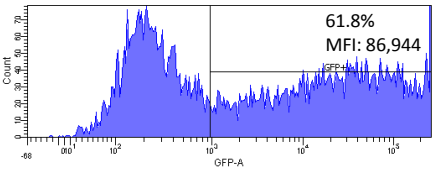

$BAX^{-/-}$ MEF

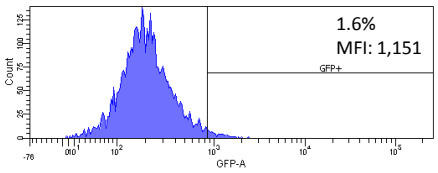

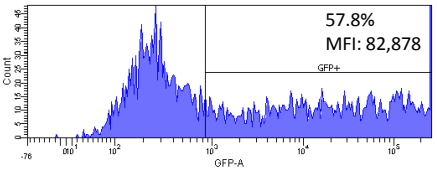

$BAK^{-/-}$ $BAX^{-/-}$ MEF

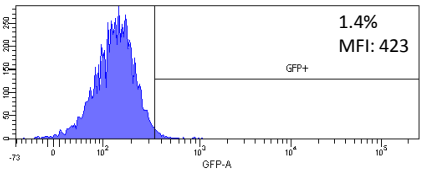

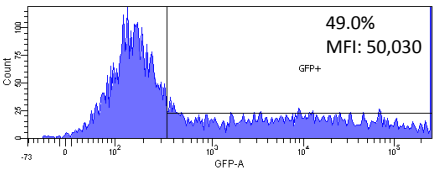

Sarosiek et al., Supplemental Figure S7

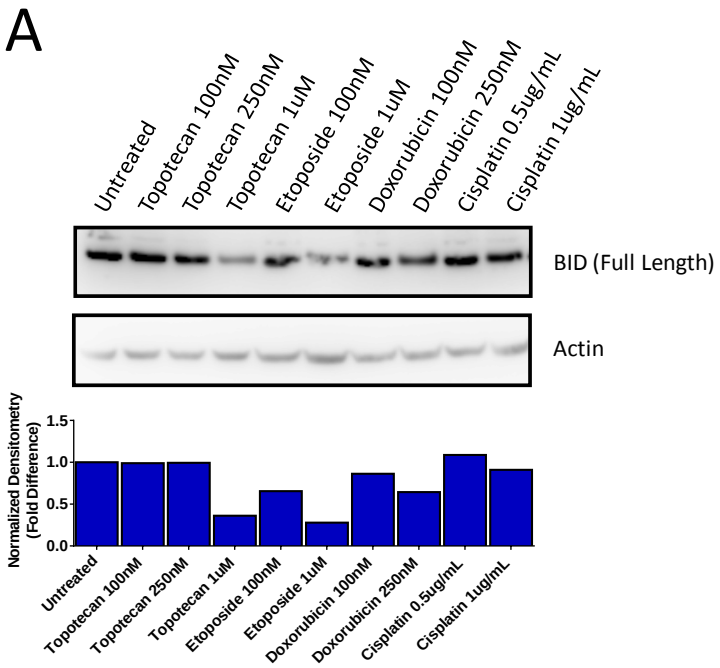

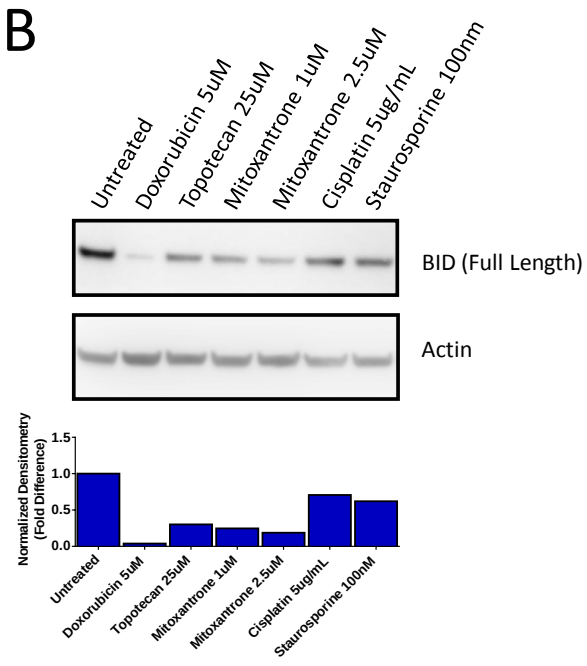

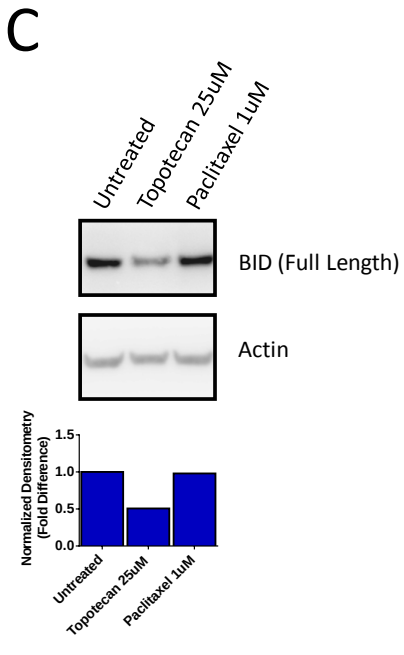

Sarosiek et al., Supplemental Figure S8

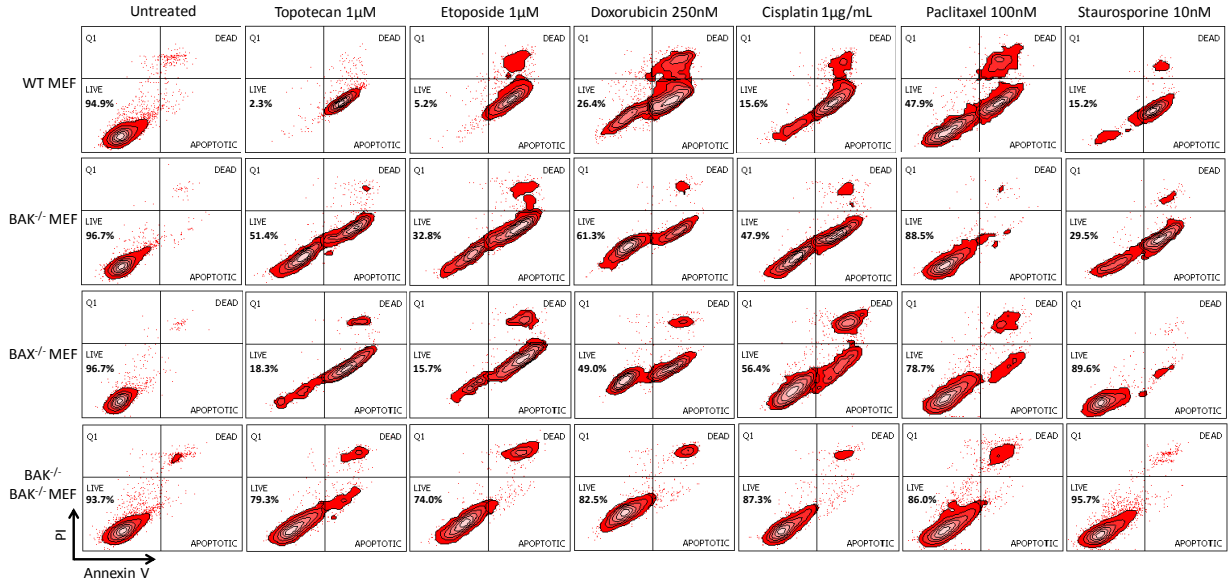

Sarosiek et al., Supplemental Figure S9

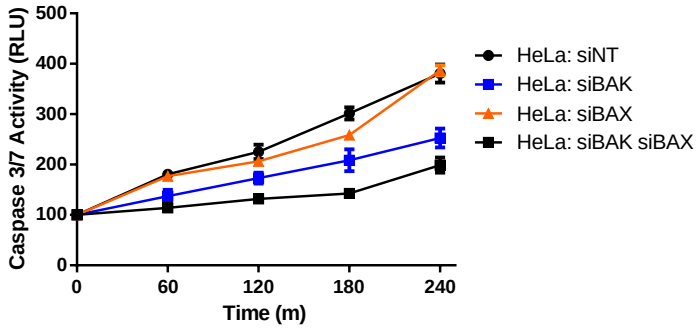

SUPPLEMENTAL FIGURE LEGENDS

Supplemental Figure S1, related to Figure 1 and 2: Densitometry of expression of BCL2 family members in MEFs and BMKs. (A) Western blotting was performed for the indicated proteins in MEFs (A) or BMKs (B). Blots were subsequently analyzed by densitometry and normalized to expression of actin. Mean ± SE, 2 IEs.

Supplemental Figure S2, related to Figure 1: Dose-response curve of BIM and BID BH3 peptides in WT MEFs. Digitonin-permeabilized MEFs were treated with indicated doses of BH3 peptides and mitochondrial potential was measured. Representative, 3 IEs.

Supplemental Figure S3, related to Figure 1: Inhibition of anti-apoptotic proteins within MEFs enhances activation preferences. Digitonin-permeabilized MEFs were pre-treated with PUMA2A (control) or PUMA (binds and inactivates major anti-apoptotic proteins including BCL-2, BCL-XL, BCL-w, MCL-1 and BFL-1) peptide which for 5 minutes. MEFs were then treated with BH3 peptides and mitochondrial polarization was monitored for 180 minutes. For each MEF, depolarization curves are shown and percent depolarization is calculated as the area under each curve compared to FCCP (positive control). In WT MEFs, PUMA pretreatment accelerated the rate of MOMP induction by the BID peptide but did not affect MOMP induced by the BIM BH3 suggesting that this peptide is less bound and sequestered by anti-apoptotic proteins than BID BH3. In the $BAK^{-/-}$ MEFs, PUMA pretreatment didn't alter the response to BIM peptide but the cells remained unresponsive to BID peptide, suggesting that the differences in MOMP induction in these cells is due to differences in BID and BIM's ability to activate BAK and BAX directly and not just inhibit anti-apoptotic proteins. In the $BAX^{-/-}$ MEFs, PUMA pretreatment again accelerated MOMP in response to BID but didn't change the response to BIM. The differences in the peptides here are even larger than what is seen in BAX KO MEFs without

PUMA pretreatment (Figure 1B). These data again suggest that the presence of anti-apoptotic proteins is not responsible for the differences we see in MOMP activation by BID and BIM and that BID and BIM instead differ in their abilities to activate BAK and BAX. Representative, % depolarization is mean ± SD, 2 IEs.

Supplemental Figure S4, related to Figure 3: HeLa cells express less BAK and BAX than MEFs. Western blotting was performed for the indicated proteins. Representative, 2 IEs.

Supplemental Figure S5, related to Figure 4: Recombinant BAX in IVTT buffer is more efficiently activated by BIM. Mitochondrial polarization was monitored in digitonin-permeabilized $BAX^{-/-}$ $BAK^{-/-}$ MEFs while initially treated for 10 minutes in the presence of recombinant BAX in IVTT buffer. BIM or BID BH3 peptides were then spiked in (arrow) and mitochondrial polarization continued to be monitored. Representative, 2 IEs.

Supplemental Figure S6, related to Figure 5: Transfection efficiencies in MEFs. MEFs of the indicated genotypes were transfected with pCMV-GFP plasmid as described in Experimental Procedures. After 24 hours, cells were collected and flow cytometry was performed to measure the level of GFP expression in cells. Representative, 2 IEs.

Supplemental Figure S7, related to Figure 6: Topoisomerase inhibitor treatment activates BID in MEFs and HeLa cells. (A) WT MEFs were treated with the indicated concentrations of agents for 48 hours and western blotting was peformed for the indicated proteins. (B-C) HeLa cells were treated with the indicated concentration of agents for either 24 (B) or 48 (C) hours (corresponding to the duration of treatment utilized in viability experiments) and western blotting was performed for the indicated proteins. (A-C) Densitometry was performed on the blots to quantify differences. Representative, 2 IEs.

Supplemental Figure S8, related to Figure 6: Resistance to topoisomerase inhibitors in BAK$^{-/-}$ cells is due to lower rates of apoptosis. MEFs were treated with the indicated compounds for 48 hours and viability was assessed by staining cells with Annexin V (apoptotic cells) and PI (dead cells) and flow cytometric analysis. Representative, 2 IEs.

Supplemental Figure S9, related to Figure 6: Knockdown of BAK attenuates TRAIL-induced activation of Caspases 3/7 in HeLa cells. HeLa cells were transfected with siRNA for the indicated gene(s) and, 48 hours later, were treated with cycloheximide and TRAIL. Caspase 3/7 activity was measured every 60 minutes with Caspase 3/7 Glo reagent. Representative, 2 IEs.

SUPPLEMENTAL TABLE LEGENDS

Supplemental Table S1, related to Figure 1: Comparison of key parameters governing mitochondrial permeabilization mediated by BID BH3 and BIM BH3 in BAK$^{-/-}$ and BAX $^{-/-}$ MEF mitochondria. BAK$^{-/-}$ and BAX$^{-/-}$ MEF mitochondrial depolarization data from Figure 1D were normalized to estimate the percentage of depolarization at each time point (see Methods). Normalized curves were fit to the equation:

$$F([\mathrm{BH3}], t) = 1 - F_{max}\left(1 - e^{-k[BH3]^m t}\right)^n$$

describing depolarization kinetics (see Methods). EC50 curve fits were performed on the fitted values of the F_{max} parameter describing the maximum depolarization at each BH3 peptide concentration in BAK$^{-/-}$ and BAX$^{-/-}$ cells. Ranges given for *k* indicate the standard error of the fitted value.

Supplemental Table 2, related to Figure 7: Comparison of clinical features in BAK$^{+/+}$ and BAK$^{+/-}$ or BAK$^{-/-}$ patients treated with topoisomerase inhibitors.

SUPPLEMENTAL TABLES

Supplemental Table S1

Comparison of key parameters governing mitochondrial permeabilization mediated by BID BH3 and BIM BH3 in BAK$^{-/-}$ and BAX $^{-/-}$ MEF mitochondria.

	EC50 (μM)		*k* (% depolarized μM^{-c} min^{-1})		F_{max} EC50 (μM)	
	BIM BH3	BID BH3	BIM BH3	BID BH3	BIM BH3	BID BH3
BAX $^{-/-}$	6.7	0.54	0.036 ± 0.002	0.115 ± 0.004	0.53	0.137
BAK $^{-/-}$	2.3	9.3	0.021 ± 0.001	0.017 ± 0.001	0.696	4.512

Supplemental Table S2

Comparison of clinical features in $BAK^{+/+}$ and $BAK^{+/-}$ or $BAK^{-/-}$ patients treated with topoisomerase inhibitors.

BAK1 Status	No. of Patients	Median Age at Diagnosis	Anatomic Organ Subdivision	Tumor Residual Disease at Diagnosis	Tumor Stage at Diagnosis	Stage III Subdivision	p53 Status at Diagnosis
+/+	142	57.5	Right or Left = 30 (21%) Bilateral = 80 (56%) Unknown = 32 (23%)	No Macroscopic disease = 19 (13.3%) 1-10 mm = 77 (54.2%) 11-20 mm = 10 (7.0%) >20 mm = 28 (19.7%) Unknown = 8 (5.6%)	Stage I = 2 (1.4%) Stage II = 6 (4.2%) Stage III = 113 (79.6%) Stage IV = 19 (13.3%) Unknown = 2 (1.4%)	Stage IIIA = 3 (2.6%) Stage IIIB = 8 (7.1%) Stage IIIC = 102 (90.2%)	Mutation: 75 (52.8%) Homozygous Deletion: 1 (0.7%) Amplification = 1 (0.7%) Amplification & Mutation = 1 (0.7%)
+/- or -/-	43	58	Right or Left = 9 (21%) Bilateral = 23 (53%) Unknown = 11 (26%)	No Macroscopic disease = 5 (11.6%) 1-10 mm = 20 (46.5%) 11-20 mm = 4 (9.3%) >20 mm = 11 (25.5%) Unknown = 3 (7.0%)	Stage I = 0 (0.0%) Stage II = 1 patient (2.3%) Stage III = 36 (83.7%) Stage IV = 6 (14.0%) Unknown = 0 (0.0%)	Stage IIIA = 0 (0%) Stage IIIB = 1 (2.7%) Stage IIIC = 35 (97.2%)	Mutation: 27 (62.8%) Homozygous Deletion: 0 (0.0%) Amplification = 0 (0.0%) Amplification & Mutation = 0 (0.0%)

SUPPLEMENTAL EXPERIMENTAL PROCEDURES

Cells and culture conditions: MEFs were cultured in Dulbecco's Modified Eagle Media (DMEM) (Life Technologies, Grand Island NY) supplemented with 10% fetal bovine serum (Life Technologies), 1% penicillin/streptomycin (Life Technologies), and 1% L-glutamine (Life Technologies). BMK cells were cultured in DMEM supplemented with 10% FBS, 1X non-essential amino acids (Life Technologies) and 1% penicillin/streptomycin. HeLa cells were cultured in RPMI 1640 media (Life Technologies) supplemented in an identical manner as the DMEM media above.

Production and purification of cBID, BIM_L, BAX and BAK: cBID was produced as previously described(Zha, 2000) with these modifications: 1) BID was cloned into pet16b; 2) cBID was eluted from the column with imidazole. For BIM_L, *the cDNA encoding* full-length wildtype murine BIM_L was cloned into pBluescript II KS(+) vector (Stratagene, Santa Clara CA). DNA sequences encoding a polyhistidine tag followed by a TEV protease recognition site (MHHHHHHGGSGGTGGSENLYFQGT) and *an intein/chitin-binding domain* were added to the plasmid such that the new plasmid encoded a fusion protein with both an N-terminal His tag and Tev site and *an intein/chitin-binding domain at the C-terminus of* BIM_L. The recombinant construct was expressed in SoluBL21 *Escherichia coli* strain (Genlantis, San Diego CA). Lysis of *E. coli* was achieved by mechanical disruption with a French p*ress. After affinity chromatography with a chitin column, intein self-cleavage and release of* BIM_L *from its fusion partner intein-CBD was initiated by incubation with buffer containing 100 mM β-mercaptoethanol for 36 h. This process leaves no additional amino acid residues on the C-terminus of* BIM_L*. The elution fraction from chitin column was then applied to a Nickel*-NTA column (Qiagen, Valencia CA) and BIM_L was eluted from the Ni column with buffer containing 20mM HEPES (pH7.4), 100mM NaCl, 20% glycerol, 0.3%CHAPS, and 300mM imidazole. The purified BIM_L protein was dialyzed against 20 mm HEPES (pH 7.4), 100mM NaCl and 20% glycerol, then flash-frozen and

stored at –80 °C. Recombinant BAX was produced as previously described(Suzuki et al., 2000). To produce BAK, in vitro transcription and translation (IVTT) reactions were performed using TnT T7 Quick Coupled Transcription/Translation System (Promega) according to manufacturer's instructions with the pcDNA3-myc-BAK plasmid.

Western blotting: Western blotting was performed as previously described(Sarosiek et al., 2009). Membranes were probed with antibodies to BAK (Millipore, Billerica MA), BAX (Cell Signaling Technologies, Danvers MA), BIM (Millipore), BID (clone 11958), BCL-2 (BD Pharmingen, San Jose CA), BCL-X_L (Cell Signaling Technologies), MCL-1 (Rockland Immunochemicals, Gilbertsville PA), and Actin (Millipore).

Crosslinking: Proliferating cells were harvested and mitochondria were isolated by performing dounce homogenization (Kontes Glass, Vineland NJ) in mitochondrial isolation buffer (250 mM sucrose, 10 mM Tris-HCl [pH 7.4], 0.1 mM EGTA). Mitochondria were pelleted and resuspended in mitochondrial experimental buffer (125 mM KCl, 10 mM Tris-MOPS [pH 7.4], 5 mM glutamate, 2.5 mM malate, 1 mM KPO_4, 10 μM EGTA-Tris [pH 7.4]) and treated with BH3 peptides at indicated concentrations for 20 minutes at 37^{o}C. 1mM 1,6-bismaleimidohexane (Thermo Fisher Scientific) was added for an additional 10 minutes at 37^{o}C and the crosslinking was quenched with 50mM Dithiothreitol (Life Technologies). 4X NuPage loading buffer (Life Technologies) was added to each sample and western blotting was performed as described above. Densitometry analysis was performed using ImageJ image analysis software (U. S. National Institutes of Health, Bethesda MD).

Ovarian cancer copy number alterations, treatment history and survival: Treatment history and survival data (clinical follow-up) for all TCGA high-grade serous ovarian adenocarcinoma cases was obtained from the TCGA data portal on August 1, 2012. Survival data was available for 567

patients while chemotherapy treatment history data was available for 518 patients. A subset of 185 patients that were treated with topoisomerase inhibitors (topotecan, etoposide, mitoxantrone and doxorubicin) was identified as well as patient subsets receiving gemcitabine (but not topoisomerase inhibitor), or carboplatin and paclitaxel alone (no gemcitabine or topoisomerase inhibitor). Copy number analysis for *BAK1*, *BAX*, *BID* and *BCL2L11* (BIM) genes was obtained via the cBIO Cancer Genomics Portal(Cerami et al., 2012) by querying the "Ovarian Serous Cystadenocarcinoma (TCGA, Nature 2011)" dataset with the following queries:

BAK1: homdel hetloss

BAX: homdel hetloss

BCL2L11: homdel hetloss

BID: homdel hetloss

The queries were performed in the subset of patients receiving topoisomerase inhibitors as well as other patient subsets included in Figure 7. Overall survival was then compared using GraphPad Prism 6 software (GraphPad Software, San Diego CA) as shown in Figure 7.

Kinetic analysis of depolarization curves: $BAK^{-/-}$ and $BAX^{-/-}$ MEF mitochondrial depolarization data were normalized to reference curves to estimate the percentage of depolarization at each timepoint. The reference curve was chosen as the most noise-free of the DMSO, 10nM peptide and 30nM peptide curves since these curves all displayed similar levels of depolarization. For the $BAK^{-/-}$ MEF + BIM BH3 condition, the $BAK^{-/-}$ + 10 nM BIM BH3 curve was used; for $BAK^{-/-}$ MEF + BID BH3 condition the $BAK^{-/-}$ + 10 nM BID BH3 curve; for $BAX^{-/-}$ MEF + BIM BH3 the $BAX^{-/-}$ + 10 nM BIM BH3 curve; and for $BAX^{-/-}$ + BID BH3 the $BAX^{-/-}$ + 30 nM BID BH3 curve. Curves were normalized according to the equation

$$N(t) = [F(t) - \min(FCCP)] / [R(t) - \min(FCCP)]$$

where N(t) is the value of the normalized curve, F(t) is the fluorescence value of the curve to be normalized, min(FCCP) is the minimum fluorescence value recorded for the FCCP condition; and R(t) is the fluorescence value of the chosen reference curve. The normalized curves were fit to the equation shown in table legend 2 by the Levenberg-Marquardt algorithm in Graphpad Prism 6 software. For the fitting procedure F_{max} and n were fit to distinct values for each curve; k was fit globally to all concentration curves for each cell line/BH3 combination; and m was manually fixed to values for each cell line that allowed robust fits for the other parameters.

Membrane permeabilization assays: Membrane permeabilization assays with liposomes encapsulating ANTS (8-Aminonaphthalene-1,3,6-Trisulfonic Acid, Disodium Salt) and DPX (p-Xylene-Bis-Pyridinium Bromide) were carried out as described previously(Billen et al., 2008; Shamas-Din et al., 2013). The liposomes used were 100 nm in diameter with a lipid composition made up of phosphatidylcholine (48%), phosphatidylethanolamine (28%), phosphatidylinositol (10%), dioleoyl phosphatidylserine (10%), and tetraoleoyl cardiolipin (4%) (all from Avanti Polar Lipids, Alabaster AL). For mitochondrial assays, mitochondria were isolated from the livers of wildtype and $BAK^{-/-}$ mice and outer membrane permeabilization of mitochondria was assessed by measuring cytochrome c release as described previously(Shamas-Din et al., 2013). Immunoblots were analyzed using ImageJ software. The curves were fit using Graphpad Prism 5 software.

Cell Viability and caspase activation Assays and Transfections: For transfections, proliferating cells were plated in 96-well plates for 24 hours and then transfected in triplicate using Lipofectamine 2000 (Life Technologies) with the following plasmids: pCMV-GFP (Addgene

plasmid 11153; Addgene, Cambridge MA)(Matsuda and Cepko, 2004), pCMV-tBID (Addgene plasmid 21149)(Li et al., 1998) and pCMV-BIM_{EL} (Addgene plasmid 23090)(Hübner et al., 2008). To test transfection efficiency, GFP expression was measured via flow cytometry on a BD LSR Fortessa Analyzer (BD Biosciences, San Jose CA). For drug-induced chemosensitivity assays, proliferating MEFs and BMKs were plated in 96-well plates and, 24 hours later, were treated with the indicated concentrations of Topotecan (Sigma-Aldrich), Etoposide (Sigma-Aldrich), Doxorubicin (Sigma-Aldrich), Cisplatin (Sigma-Aldrich), Paclitaxel (Sigma-Aldrich), Mitoxantrone (Sigma-Aldrich) and Staurosporine (Sigma-Aldrich) for 24 or 48 hours. Treatments with super killer TRAIL (Enzo Life Sciences, Farmingdale NY) were done in the presence of cycloheximide (Sigma-Aldrich) to prevent TRAIL's pro-survival effects(Thakkar et al., 2001). Cell Titer Glo Assay (Promega, Madison WI) was then performed according to manufacturer's instructions and luminescence was measured on a Safire2 microplate reader (Tecan, Männedorf Switzerland). Luminescence readings were normalized to DMSO (vehicle) treated control cells except TRAIL-treated wells which were normalized to cycloheximide-only control cells. For Annexin V/PI assessment of viability MEFs were plated in 48-well plates and, 24 hours later, treated with chemotherapy agents. 48 hours later cells were collected and stained with Annexin V-FITC (prepared in our lab) and Propidium Iodide (Sigma-Aldrich). Annexin V/PI positivity was assessed via flow cytometry on a BD LSR Fortessa Analyzer (BD Biosciences). For viability and BH3 profiling assays, HeLa cells were transfected using RNAi Max reagent (Invitrogen) according to manufacturer's instructions with non-targeting siRNA or siRNA targeting human BAX and/or BAK (Dharmacon, Lafayette CO). 48 hours later cells were either BH3 profiled or were treated with indicated chemotherapies for an additional 24 or 48 hours, after which the viability was assayed as described above using Cell Titer Glo Assay. Caspase 3/7 activity was measured using Caspase 3/7 Glo assay according to manufacturer's instructions (Promega).

Statistical Analysis: EC50 determination, two-way ANOVA (Fisher's LSD test), Pearson correlation coefficient (r) and Kaplan-Meier survival analysis (with Log-Rank test) were performed using the GraphPad Prism software (GraphPad Software). Significance: * $p < 0.05$; ** $p < 0.01$; *** $p < 0.001$; **** $p < 0.0001$.

SUPPLEMENTAL REFERENCES

Billen, L.P., Kokoski, C.L., Lovell, J.F., Leber, B., and Andrews, D.W. (2008). Bcl-XL inhibits membrane permeabilization by competing with Bax. PLoS Biology *6*, e147.

Cerami, E., Gao, J., Dogrusoz, U., Gross, B.E., Sumer, S.O., Aksoy, B.A., Jacobsen, A., Byrne, C.J., Heuer, M.L., Larsson, E., et al. (2012). The cBio Cancer Genomics Portal: An Open Platform for Exploring Multidimensional Cancer Genomics Data. Cancer Discovery *2*, 401–404.

Hübner, A., Barrett, T., Flavell, R.A., and Davis, R.J. (2008). Multisite phosphorylation regulates Bim stability and apoptotic activity. Molecular Cell *30*, 415–425.

Li, H., Zhu, H., Xu, C.J., and Yuan, J. (1998). Cleavage of BID by Caspase 8 Mediates the Mitochondrial Damage in the Fas Pathway of Apoptosis. Cell *94*, 491–501.

Matsuda, T., and Cepko, C.L. (2004). Electroporation and RNA interference in the rodent retina in vivo and in vitro. Proceedings of the National Academy of Sciences of the United States of America *101*, 16–22.

Sarosiek, K. a, Nechushtan, H., Lu, X., Rosenblatt, J.D., and Lossos, I.S. (2009). Interleukin-4 distinctively modifies responses of germinal centre-like and activated B-cell-like diffuse large B-cell lymphomas to immuno-chemotherapy. British Journal of Haematology *147*, 308–318.

Shamas-Din, A., Bindner, S., Zhu, W., Zaltsman, Y., Campbell, C., Gross, A., Leber, B., Andrews, D.W., and Fradin, C. (2013). tBid undergoes multiple conformational changes at the membrane required for Bax activation. The Journal of Biological Chemistry.

Suzuki, M., Youle, R.J., and Tjandra, N. (2000). Structure of Bax: coregulation of dimer formation and intracellular localization. Cell *103*, 645–654.

Thakkar, H., Chen, X., Tyan, F., Gim, S., Robinson, H., Lee, C., Pandey, S.K., Nwokorie, C., Onwudiwe, N., and Srivastava, R.K. (2001). Pro-survival function of Akt/protein kinase B in prostate cancer cells. Relationship with TRAIL resistance. The Journal of Biological Chemistry *276*, 38361–38369.

Zha, J. (2000). Posttranslational N-Myristoylation of BID as a Molecular Switch for Targeting Mitochondria and Apoptosis. Science *290*, 1761–1765.